RSC Advances

Hybrid electrolyte Li-air rechargeable batteries base on the Nitrogen- and Phosphorus-doped graphene nanosheets

Journal:	*RSC Advances*
Manuscript ID:	RA-COM-01-2014-000809.R1
Article Type:	Communication
Date Submitted by the Author:	24-Feb-2014
Complete List of Authors:	Yoo, Eunjoo; AIST, Energy technology Research Group Zhou, HaoShen; AIST,

Journal Name

RSCPublishing

COMMUNICATION

Hybrid electrolyte Li-air rechargeable batteries base on the Nitrogen- and Phosphorus-doped graphene nanosheets

Cite this: DOI: 10.1039/x0xx00000x

E. J. Yoo and H. Zhou*

Received ooth January 2012,
Accepted ooth January 2012

DOI: 10.1039/x0xx00000x

www.rsc.org/

The nitrogen doped GNSs (N-doped GNSs) and phosphorus doped GNSs (P-doped GNSs) are examined as a cathode electrode for hybrid electrolyte Li-air battery in basic condition. The N-doped GNSs not only show a high discharge voltage that is near that of 20wt%Pt/carbon black, but also provide better rate performance in discharge process than that of the P-doped GNSs.

Li-air batteries have become promising candidates for electric devices such as mobile phones, laptops and electric vehicles due to therein extremely high theoretical energy density (theoretical value of 3600 Wh/kg).[1] However, there are some serious problems in the Li-air batteries with non-aqueous electrolyte, the solid discharge product is insoluble in the organic electrolyte, and the organic electrolyte decompose during discharge and charge process, resulting in the formation of Li_2CO_3.[2,3] Our group reported that the hybrid electrolyte Li-air batteries overcomes the drawbacks of non-aqueous Li-air batteries.[4] However, optimization of the air electrode is still needed, which plays an important role in electrochemical performance of hybrid electrolyte Li-air batteries, to improve the cell performance in this Li-air system, because the air electrode revealed poor cycle performance and durability. Thus, it is still a critical challenge to develop an optimal cathode catalyst for Li-air batteries.

Recently, graphene nanosheets (GNSs) have been reported as a good candidate for cathode catalysts in the Li-air batteries because of their unique morphology structure, good electroconductivity and high specific surface area.[5,6] Our group has already proposed that the GNSs have the good potential as cathode electrode for Li-air batteries with hybrid electrolyte.[7] Furthermore, it is reported that the N-and P-doped carbons such as carbon nanotubes (CNTs) and graphene as a metal free catalyst had a good activity of oxygen reduction reaction (ORR) in alkaline and acidic media.[8,9] Recent studies also demonstrated effect of the single or binary doping of heteroatom (N, and P) into the carbon structure for ORR.[10]

Chemical doping with foreign atoms is a common approach to tailor the electronic properties of carbon materials. For instance, after doping with N and P or B atoms, carbon materials become n-type and p-type, respectively.[11,12] Previous reports have proposed that chemical doping with N and P atom into the carbon can modify the electric property, and enhance the interaction between carbon and N and P, thus improve the electrochemical performance of various devices such as fuel-cell, Li-air batteries, supercapacitors, and etc.[13-15] However, despite such significant advantages, there is little report about the application of other element doped carbon as cathode catalysts for Li-air batteries. Furthermore, the mechanism of ORR for other element doped carbon is still unclear. Therefore, it is important to understand the effect of the physical characteristics of the chemical doping with N and P atom into the carbon materials.

In this study, we report the electrochemical performance of N-doped GNSs and P-doped GNSs, which have the same n-type behaviour, for Li-air batteries with hybrid electrolyte under basic condition and further investigate the reason of differences in electrochemical activity based on X-ray photoelectron spectroscopy (XPS) studies of the modified materials.

Table 1 BET surface area and composition ratio of N/C and P/C of N-doped GNSs and P-doped GNSs.

	BET surface Area/ m^2g^{-1}	The atomic concentration by integrating XPS peak		
		C	N or P	N/C or P/C ratio
N-doped GNSs	227.8	96.4%	1.6%	0.017
P-doped GNSs	198.7	95.3%	2.0%	0.021

The BET surface area and composition ratio of N/C, P/C of N-doped GNSs and P-doped GNSs used in this study are summarized in Table 1. The BET surface area of N-doped GNSs and P-doped GNSs are measured to be 227.8 and 198.7 m^2g^{-1}, respectively. In addition, the N and P contents for N-and P-doped GNSs, respectively, are obtained by integrating XPS peak. The relative contents of N and P are about 1.6 and 2.0 % for N-doped GNSs and P-doped GNSs. The N/C and P/C ratio also is calculated based on the atomic concentration of N_{1s}, P_{2p} and C_{1s} by integrating XPS peak. The N/C and P/C ratio is about 0.017 and 0.021 for N-doped GNSs and P-doped GNSs, respectively.

Figure 1 is a schematic structure of the Li-air battery with a hybrid electrolyte based on N-and P-doped GNSs as air electrode. The

modification of GNSs through doping N-and P- may change the properties of GNSs and it is expected to enhance the catalytic activity of ORR. Thus, it is important to investigate which element is better as a dopant of GNSs for cathode catalysts in the Li-air batteries with hybrid electrolyte.

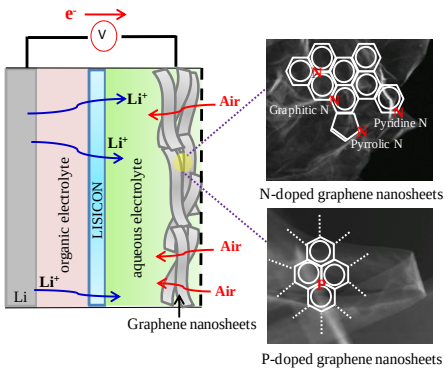

Figure 1 schematic structure of the Li-air battery with a hybrid electrolyte based on N-, and P-doped GNSs as an air electrode

Figure 2(a) shows the discharge curves of N-doped GNSs, P-doped GNSs, graphene nanosheets and 20wt%Pt/CB at a current density of 0.5 $mAcm^{-2}$ in 1 M $LiNO_3$ + 0.5 M LiOH for 24 h. The commercial 20wt%Pt/CB is investigated as a reference under the same condition to compare the electrode performance for hybrid electrolyte Li-air batteries. The discharge voltage keeps at about 3.00, 2.84, 2.94 and 3.02 V *versus* Li/Li^+ for N-doped GNSs, P-doped GNSs, graphene nanosheets and 20wt%Pt/CB, respectively. Interestingly, the discharge voltage of N-doped GNSs is near that of 20wt%Pt/CB and is 0.15 and 0.06 V higher than that of the P-doped GNSs and graphene nanosheets. Thus, it is indicated that the discharge performance influenced by type of dopants used in additional doping and the nitrogen incorporated into graphene nanosheets is more effective to improve the discharge performance in Li-air batteries with hybrid electrolyte.

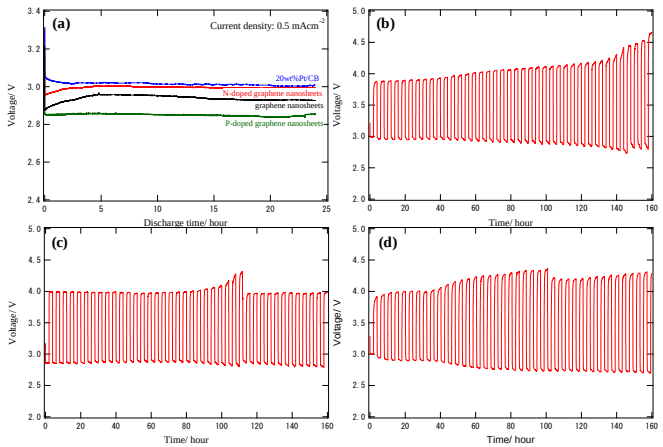

Figure 2 discharge curves of N-doped GNSs, P-doped GNSs, graphene nanosheets and 20wt%Pt/CB (a) at current density of 0.5 $mAcm^{-2}$ for 24 h, cycle performance of N-doped GNSs (b), P-doped GNSs (c), and 20wt%Pt/CB (d) at current density of 0.5 $mAcm^{-2}$ for 2 h

Figure 2 (b-d) shows the cycle performance of N-doped GNSs, P-doped GNSs and 20wt%Pt/CB at a current density of 0.5 $mAcm^{-2}$ for 1-40 cycles. All samples are discharged for 2 h and charged for another 2 h. At first cycle, the voltage gap between discharge and charge shows approximately 0.88, 1.15 and 0.91 V *versus* Li/Li^+ for N-doped GNSs, P-doped GNSs and 20wt%Pt/CB, respectively. However, with increasing numbers of charge-discharge cycles, the voltage gap of N-doped GNSs increase from about 0.88 to 1.85 V *versus* Li/Li^+ after 40th cycle. Furthermore, the voltage gap between discharge and charge of 20wt%Pt/CB at 40th cycle is about at 1.62 V *versus* Li/Li^+. On the other hand, for the P-doped GNSs, the voltage gap between discharge and charge at 40th cycle is kept about at 1.19 V *versus* Li/Li^+. It also investigated that the voltage gap of graphene nanosheets increase from 0.95 to 1.2 V *versus* Li/Li^+ after 40th cycle, although we do not show it this paper. This shows that P-doped GNSs have much more stable cycle performance than that of N-doped GNSs and 20wt%Pt/CB. J.G Radich et al., have reported that the $OH^{\cdot}$ radicals which yield from UV photolysis of H_2O_2, could lead to increased degradation of carbon support such as graphene oxide and reduced graphene oxide.[16] However, this report may be different from our case. Thus, we consider that the stable cycle performance of P-doped GNSs may be the result of changes in the surface structure of GNSs after P-doped at high temperature, which is ascribed to graphitize the surface carbon, as confirmed by TG and XRD measurement and discussed in detail below.

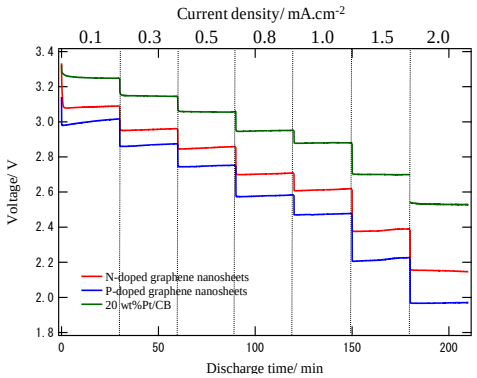

Figure 3 discharge performance with different current density in the range of 0.1 to 2.0 $mAcm^{-2}$ for 30 min

Figure 3 displays the discharge curves with different current densities of N-doped GNSs, P-doped GNSs and 20wt%Pt/CB, respectively. All measured samples are discharged at current densities in the range from 0.1 to 2.0 $mAcm^{-2}$ for 30 min. At a current density of 0.1 $mAcm^{-2}$, the discharge voltage is 3.11, 3.0 and 3.25 V *versus* Li/Li^+ for the N-doped GNSs, P-doped GNSs and 20wt%Pt/CB, respectively. The 20wt%Pt/CB is still remained the operating voltage of 2.55 V even though at a current density of 2.0 $mAcm^{-2}$. Meanwhile, for the N-doped GNSs, the operating voltage at a current density of 2.0 $mAcm^{-2}$ is 0.37 V less than that of 20wt%Pt/CB. The discharge voltage of P-doped GNSs at current density of 2.0 $mAcm^{-2}$ is 1.98 V, which 0.57 less than that of 20wt%Pt/CB. This shows that the rate performance in discharge process is depended on additional kinds of atom into graphene network. We also find that the operating cell potential for all measured samples decreased linearly with increasing current density. Previously our group suggested that decreasing the electrochemical performance with increasing current density in the Li-air battery with hybrid electrolyte is attributed to the low ionic conductivity of LISICON at a high current density.[17] We therefore considered that this phenomenon also can be due to the resistance of LISICON and due to increasing mass transfer limitations at higher current densities.

The thermal property and surface morphology of N-and P-doped GNSs are characterized by TG analysis and SEM measurement. Typical thermal curves in air flow of N-and P-doped GNSs are presented in Figure 4 (a). Figure 4 (a) shows that the N-doped GNSs is burned out at about 500-700 °C, corresponding to combustion of carbon framework. In contrast, as shown in Figure 4(a), the TG curve of P-doped GNSs shows that lost significant amounts of mass (98 %) from 670 to 800 °C as a result of combustion of the carbon framework. Figure 4 (b) shows the XRD patterns of N-doped GNSs and P-doped GNSs to clarify the graphitization degree of both samples. We can find the diffraction peaks at 26.5° attributed to the hexagonal graphite structure ((002) plane) is observed for N-doped GNSs and P-doped GNSs. The P-doped GNSs peak of graphite structure ((002) plane) for XRD pattern is sharper than that of the N-doped GNSs. The full widths at half maximum (FWHM) is estimated to be 5.2 and 2.1° for N-doped GNSs and P-doped GNSs, respectively. Thus it is considered that the P-doped GNSs displays good graphitization as it leads to restoration of the carbon framework compared to that of N-doped GNSs. The morphology of typical air cathode films is shown in Figure 4 (c) (d), examined by SEM. It can be clearly seen that the GNSs have a curled structure with wave, wrinkled and paper-like. However, there is no distinguishable difference between N-doped GNSs and P-doped GNSs films by the SEM observation.

The detailed reason of good cycle performance for the P-doped GNSs is not clear yet. However, we have found that the cycle performance significantly depends on the graphitization of carbon. It is considered that the good cycle performance of P-doped GNSs is ascribed to the good graphitization of surface carbon as shown by the XRD pattern (Figure 4b).

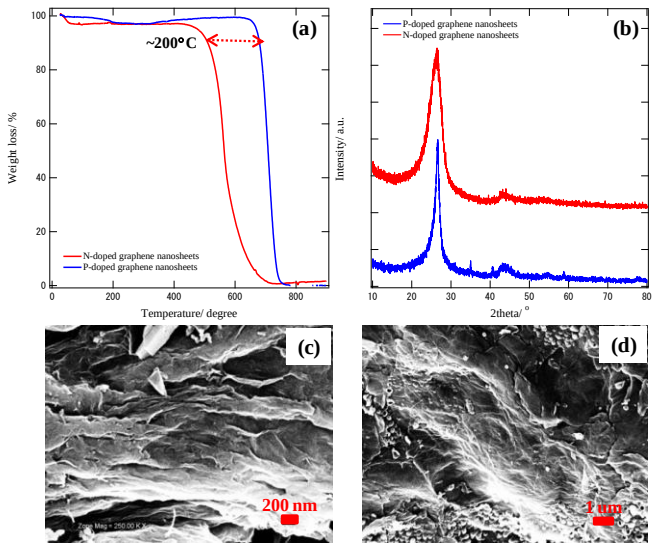

Figure 4 TG result (a), XRD result (b) and SEM images of N-doped GNSs film, (c) P-doped GNSs film (d)

The XPS spectra confirm the doping of the graphene nanosheets. Figure 5 (a) shows the N1s spectra of N-doped GNSs. The curves are deconvoluted into four peak, indicating that nitrogen atoms are in the different bonding characters inserted into the garphene network: pyridinic type N (399.3 eV), graphitic type N (401.7 eV), pyrrolic type N (400.5 eV) and N-O (403.2 eV).[18] In addition, as can be seen in Figure 5 (b), the P_{2p} XPS spectra of P-doped GNSs also show that the P_{2p} peak has four components, assign to P-P and P-O bonding according to P_{2p} peak of P-C.[19] On the basis of XPS result, we conclude that the nitrogen and phosphorus atoms have been doped into graphene network successfully.

It is reported that N-doped into carbon induces positively charged carbon atoms, results in an increase of ORR activity.[20] Meanwhile, it is suggested that P-doped into carbon cause a break of electroneutralities due to the lower electronegativity of P (2.19) than that of C (2.55), results in inducing negative charge in carbon atoms.[21] That is, the charge density of carbon due to additional N-and P-doping is very important in determining ORR activity. Figure 6 shows the XPS-C_{1s} spectra of N-doped GNSs and P-doped GNSs. The N-doped GNSs exhibit peaks of the C-C bond at 284.7 eV, which is higher binding energy of 0.2 eV than that of P-doped GNSs. Thus, it is indicated that more electrons from carbon was transferred and these electrons significantly enhance the charge delocalization at the carbon atoms by doping nitrogen into carbon atoms. Gong et al. have reported that the charge delocalization of N-doped carbon provided oxygen adsorption sites, and it is an active site for the ORR by weakening the O-O bond intensity, which is adsorbed in the carbon atoms.[21] Thus, we considered that the high discharge performance of N-doped GNSs is ascribed to enhance the charge delocalization of graphene sheets and these properties can facilitate the adsorption of O_2 leading to enhance catalytic activity of oxygen reduction reaction. Although the detailed ORR mechanism is not clear for N-doped GNSs and P-doped GNSs, we found that the discharge performance varied depending on doping with foreign atom into the GNSs. It is shown that the N-doped GNSs are expected to be a good cathode catalyst for Li-air batteries with hybrid electrolyte.

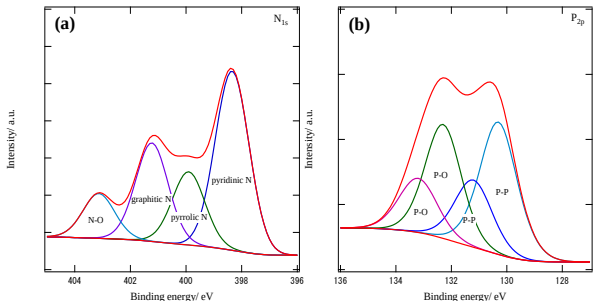

Figure 5 XPS spectra of N_{1s} (a) and P_{2p} (b) for N-doped GNSs and P-doped GNSs

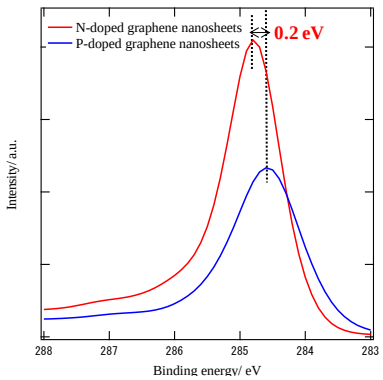

Figure 6 XPS-C_{1s} spectroscopy of N- and P-doped GNSs

Conclusions

We prepared the N-doped GNSs and P-doped GNSs for use as cathode electrodes in the hybrid electrolyte Li-air batteries under alkaline electrolyte. The N-doped GNSs show the good discharge performance and rate performance compared to the P-doped GNSs. It is considered that the N-doped on GNSs lead to change in the properties of carbon, and improve the electrochemical performance. Thus, suitable chemical doping with foreign atoms into the GNSs is the key to the enhanced electrochemical performance in the Li-air batteries with hybrid electrolyte. Further research on Li-air battery using a chemical doping with foreign atoms into the GNSs should be directed toward conform the mechanism of electrochemical reaction to improve the electrochemical performance.

Acknowledgments

This work was partially supported by Grant for Environmental Research Projects from Sumitomo Foundation. LISICON (lithium super-ion conductor glass film) is provided by the Ohara Company in Japan.

Notes and references

Energy Technology Research Institute, National Institute of Advanced Industrial Science and Technology, Umezono 1-1-1, Central 2, Tsukuba, Ibaraki 305-8568, Japan. TEL/FAX: +81-29-861-5648/+81-29-861-5799: Email:hs.zhou@aist.go.jp

† Footnotes should appear here. These might include comments relevant to but not central to the matter under discussion, limited experimental and spectral data, and crystallographic data.

Electronic Supplementary Information (ESI) available: [details of any supplementary information available should be included here]. See DOI: 10.1039/c000000x/

1 A. Armand and J.M. Tarascon, Nature, 2008, **451**, 652.
2 K.M. Abraham and Z. Jiang, J. Electrochem. Soc., 1996, **143**, 1.
3 T. Ogasawara, A. De´ bart, M. Holzapfel, K.P. Nova´ and P. G. Bruce, J. Am Chem Soc., 2006, **128**, 1390.
4 Y. Wang and H. Zhou, Journal of Power Sources, 2010, **195**, 358.
5 D. Yu, Q. Zhang and L. Dai, J. Am. Chem.Soc., 2010, **132**, 15127.
6 X. Li, H. Wang, J.T. Robinson, H. Sanchez, G. Diankov and H. Dai, J. Am. Chem.Soc., 2009, **131**, 15939.
7 E.J. Yoo and H. Zhou, ACS nano, 2011, **5**, 3020.
8 Z.W. Liu, F. Peng, H.J. Wang, H. Yu, W.X. Zheng and J.A. Yang, Angew. Chem. Int.Ed., 2011, **50**, 3257.
9 S. Chen, J. Bi, Y. Zhao, L. Yang, C. Zhang, Y. Ma, Q. Wu, X. Wang and Z. Hu, Adv. Mater., 2012, **24**, 5593.
10 C.H. Choi, S.H. Park and S.I. Woo, ACS nano, 2012, **6**, 7084.
11 K. Xiao, Y.Q. Liu, P.A. Hu. G.Yu, Y.M. Sun and D.B. Zhu, J. Am. Chem. Soc., 2005, **127**, 8614.
12 H. Terrones, M. Terrone, E. Hernandez, N. Grobert, J.C. Charlier and P.M. Ajayan. Phys. Rev. Lett., 2000, **84**, 1716.
13 Y.M. Yu, J.H. Zhang, C.H.Xiao, J.D. Zhong, X.H. Zhang and J.H. Chen, Fuel cells, 2012, **12**, 506.
14 E.J. Yoo, J. Nakamura and H. Zhou, Energy Environ. Sci., 2012, **5**, 6928.
15 D.W. Wang, F. Li, Z.G. Chen, G.Q. Li and H.M. Cheng, Chem. Mater, 2008, **20**, 7195.
16 J.G. Radich and P.K. Kamat, ACS nano, 2013, **7**, 5546.
17 P. He, Y. Wang and H. Zhou. Chem. Commun., 2011, **47**, 10701.
18 Y. Wang, D.C. Alsmeyer and R.L. McCreery, Chem. Mater, 1990, **2**, 557.
19 O.S. Panwar, M.A. Khan, M. Kumar, S.M. Shivaprasad, B.S. Satyanarayana, P.N. Dixit and R.Bhattacharyya, Jpn, J, Appl, Phys., 2009, **48**, 065501-1.
20 K.P. Gong, F. Du, Z.H. Xia, M. Durstock and L.M. Dai, Science, 2009, **323**, 760.
21 L. J. Yang, S. J. Jiang, Y. Zhao, L. Zhu, S. Chen, X. Z. Wang, Q Wu, J. Ma, Y. W. Ma and Z. Hu, Angew. Chem., Int. Ed., 2011, **50**, 7132.

